Supporting Information

ε-polylysine organic ultra-long room temperature phosphorescent materials based on phosphorescent molecules doping

Jiaying Cui[a], Syed Husnain Ali[a], Zhuoyao Shen[a], Wensheng Xu[a], Jiayi Liu[a], Pengxiang Li[a], Yang Li[*,a,c], Ligong Chen[a,b,c] ,Bowei Wang[*,a,b,c]

a School of Chemical Engineering and Technology, Tianjin University, Tianjin, 300350, P. R. China.

b Zhejiang Institute of Tianjin University, Shaoxing, 312300, P.R. China.

c Tianjin Engineering Research Center of Functional Fine Chemicals, Tianjin, 300350, P.R. China.

* Corresponding author at: School of Chemical Engineering and Technology, Tianjin University, Tianjin 300350, P. R. China.

E-mail: bwwang@tju.edu.cn (Bowei Wang, ORCID ID: 0000-0002-9400-0698);

liyang777@tju.edu.cn (Yang Li, ORCID ID: 0000-0002-5044-6049)

Experimental Section

Materials

All chemical reagents used in this work were purchased from commercial source without further purification. Polylysine (ε-polylysine, ε-PL) was purchased from Energy Chemical, polymethyl methacrylate was purchased from Shanghai D&B Biological Science and Technology Co., ltd. 9, 10-diaminophenanthrene, 2, 3-naphthalenedicarboxylic acid, 6-amino-2-naphthoic, 1-aminopyrene and 5-amino-2-naphthalenesulfonic acid were purchased from Macklin reagent Co., Ltd. Ethyl alcohol (EtOH) and dichloromethane (DCM) were purchased from Jiangtian Chemical and used directly. The pure water was provided by Hangzhou Wahaha Group Co., Ltd. for preparation of ε-polylysine solution.

Characterization

The phosphorescence lifetime, excitation-dependent emission spectra, time-dependent emission spectra, steady-state and delayed phosphorescence spectra were measured on a FLS1000

fluorescence spectrophotometer (Edinburgh Instruments, UK) equipped with a xenon lamp and a microsecond flash-lamp. Photoluminescence quantum yields were obtained on a FLS1000 fluorescence spectrophotometer (Edinburgh Instruments, UK) equipped with an integrating sphere. The lifetimes (τ) of the luminescence were obtained by fitting the decay curve with a multi-exponential decay function:

$$I(t) = \sum_i A_i e^{\frac{t}{\tau_i}}$$

where A_i and τ_i represent the amplitude and lifetime of an individual component for multiexponential decay profiles, respectively. The Φ_{Phos} measurement was conducted using a microsecond lamp as the excitation source, and the fluorescence section can be filtered out by using the gating delay system, so that more accurate Φ_{Phos} was obtained. The quantum yield measurements on FLS1000 were calculated mainly based on different phosphorescence emission spectra of reference and samples, and Φ_{Phos} was calculated by FLS1000 software.

Fourier transform infrared spectra were measured on a Nicolet 380 FT-IR spectrometer. X-ray diffraction (XRD) analyses were carried out on Bruker AXS D8 X-ray diffractometer (Germany) using a Cu Kα X-ray source with 2θ range of 10-60° (40 kV, 100 mA). SEM images were taken by a field emission scanning electron microscopy (Japan). Thermogravimetric analysis (TGA) was carried out NETZSCH TG 209 F3 in nitrogen atmosphere from 40 to 800 ºC with a ramping rate of 10 ºC min^{-1}. Differential scanning calorimetry (DSC) was conducted on NETZSCH DSC 214 at a heating rate of 10 ºC / min under nitrogen. High resolution mass spectrum (HRMS) was recorded on a Bruker Daltonics Autoflex III instrument (America). Density functional theory (DFT) calculations were performed using Gaussian 09 software package at the M06-2X / 6-311g (d, p) level. Natural transition orbit (NTO) calculations were performed using Multiwfn software package.

Preparation of polymer-based afterglow materials

1. ε-PL-based afterglow materials

ε-PL (500.0 mg) was added to deionized water (10 mL), and the ε-PL solution was stirred at room temperature for 30 minutes. Similarly, 9,10-Diaminophenanthrene (5 mg) was added to ethanol (5 mL), and the 9,10-Diaminophenanthrene solution was stirred at room temperature for 30 minutes, too. Subsequently, mixed the two prepared solutions together. The resulting mixture was stirred at 50 °C for 1 hour, then concentrated to about 3-5 mL, and finally dried to form a film. The

others were also prepared as described above.

2. PMMA-based afterglow materials

PMMA (500.0 mg) was added to dichloromethane (5 mL), and the PMMA solution was stirred at room temperature for 30 minutes. Similarly, 9,10-Diaminophenanthrene (5 mg) was added to ethanol (5 mL), and the 9,10-Diaminophenanthrene solution was stirred at room temperature for 30 minutes, too. Subsequently, mixed the two prepared solutions together. The resulting mixture was stirred at 50 ℃ for 1 hour, then concentrated to about 3-5 mL, and finally dried to form a film. The others were also prepared as described above.

3. ε-PL-based afterglow materials without functional groups in small molecules

ε-PL (500.0 mg) was added to deionized water (10 mL), and the ε-PL solution was stirred at room temperature for 30 minutes. Similarly, phenanthrene (5 mg) was added to ethanol (5 mL), and the phenanthrene solution was stirred at room temperature for 30 minutes, too. Subsequently, mixed the two prepared solutions together. The resulting mixture was stirred at 50 ℃ for 1 hour, then concentrated to about 3-5 mL, and finally dried to form a film. The others were also prepared as described above.

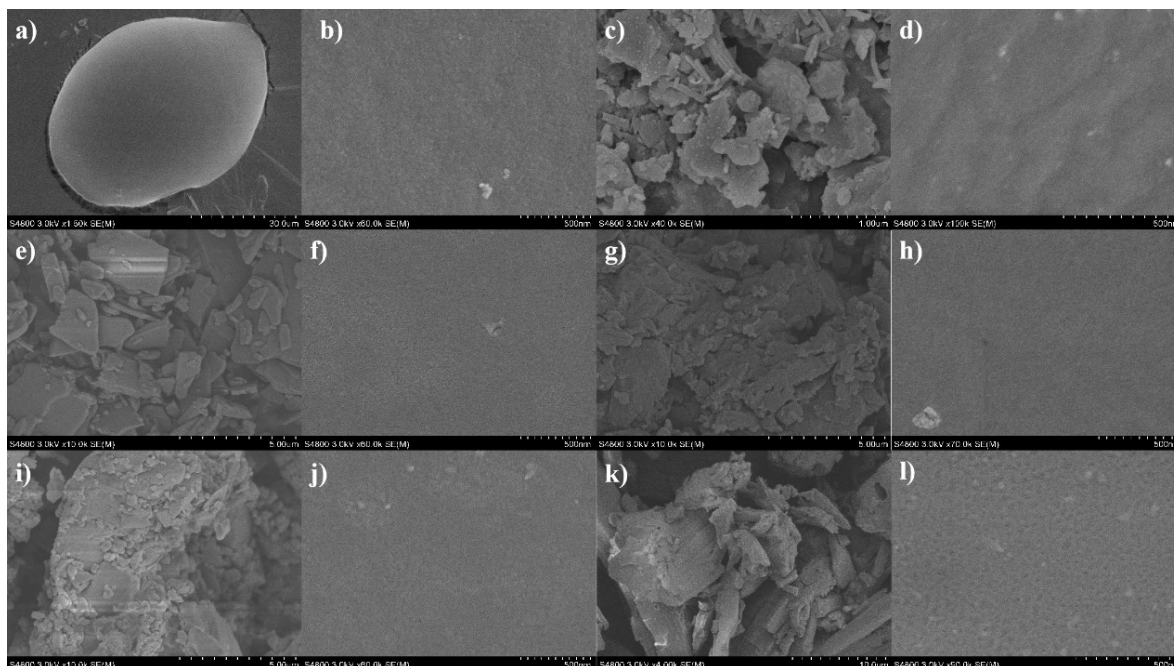**Supplementary figures and tables**

Figure S1. SEM images of raw materials and films. The first and third columns were the solid powder of the raw material, and the second and fourth columns were the films. (a) ε-PL powder, (b) ε-PL film, (c) Daphe, (d) Daphe@ε-PL, (e) NDA, (f) NDA@ε-PL, (g) ANA, (h) ANA@ε-PL, (i) ANS, (j) ANS@ε-PL, (k) Apyr, (l) Apyr@ε-PL

It can be seen from the SEM images that the small molecules showed irregular flaky appearance before doping, and uniform smooth films after doping, indicating that the small molecules were successfully doped into ε-PL.
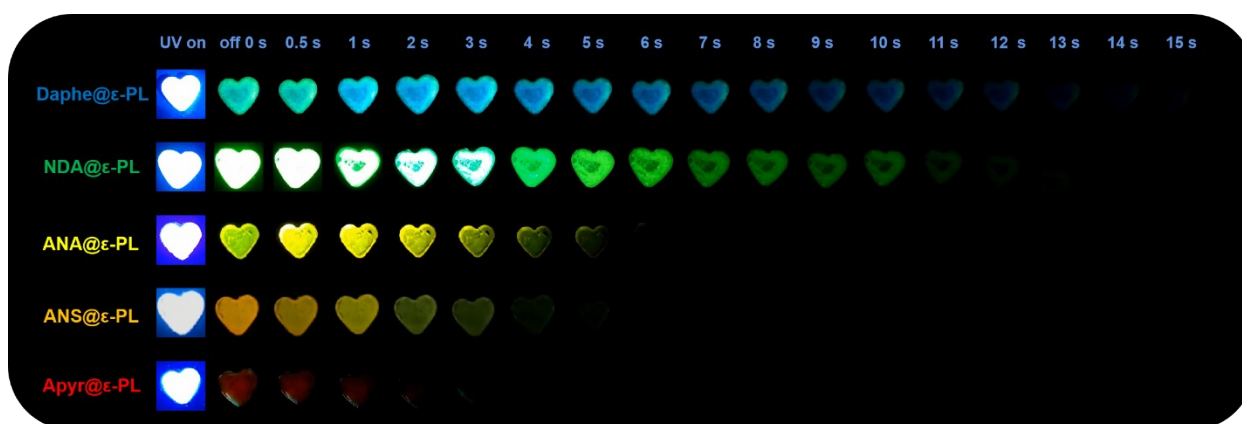
Figure S2. Photographs of ε-PL-based afterglow films taken under 365 nm UV light and after ceasing.
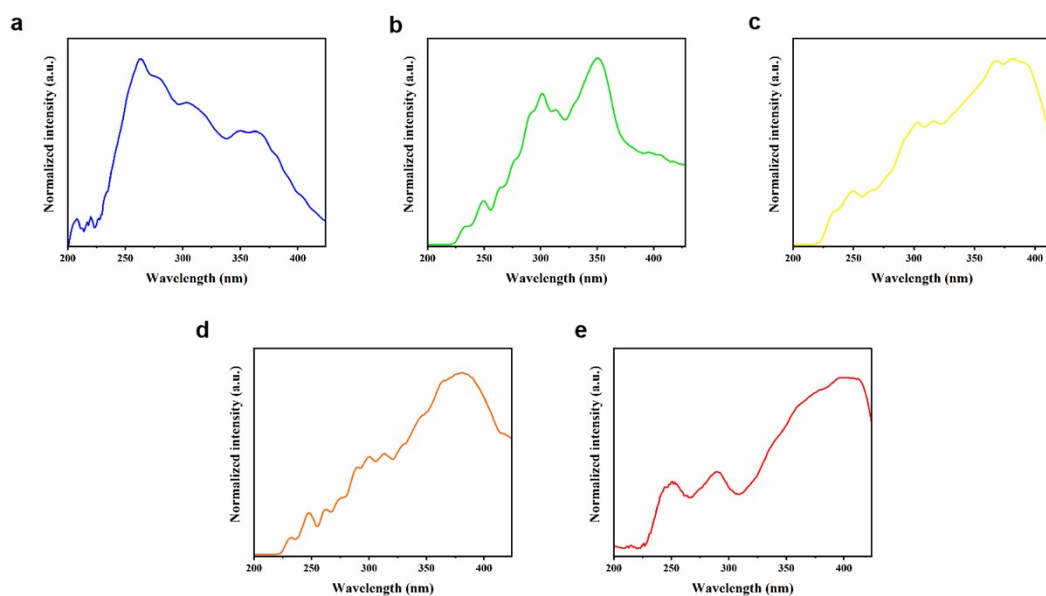
Figure S3. The excitation spectra of five materials. (a) Daphe@ε-PL, (b) NDA@ε-PL, (c) ANA@ε-PL, (d) ANS@ε-PL, and (e) Apyr@ε-PL.
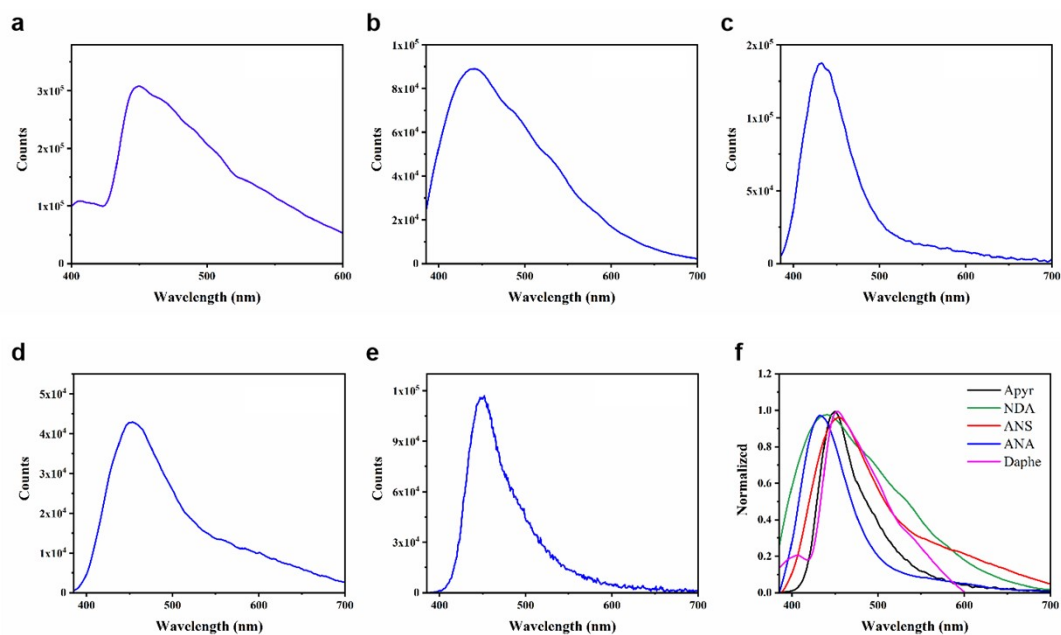

Figure S4. The photoluminescence spectra of five materials. (a) Daphe@ε-PL (λem = 450 nm), (b) NDA@ε-PL (λem = 448 nm), (c) ANA@ε-PL (λem = 433 nm), (d) ANS@ε-PL (λem = 454 nm), and (e) Apyr@ε-PL (λem = 450 nm). (f) Summary chart
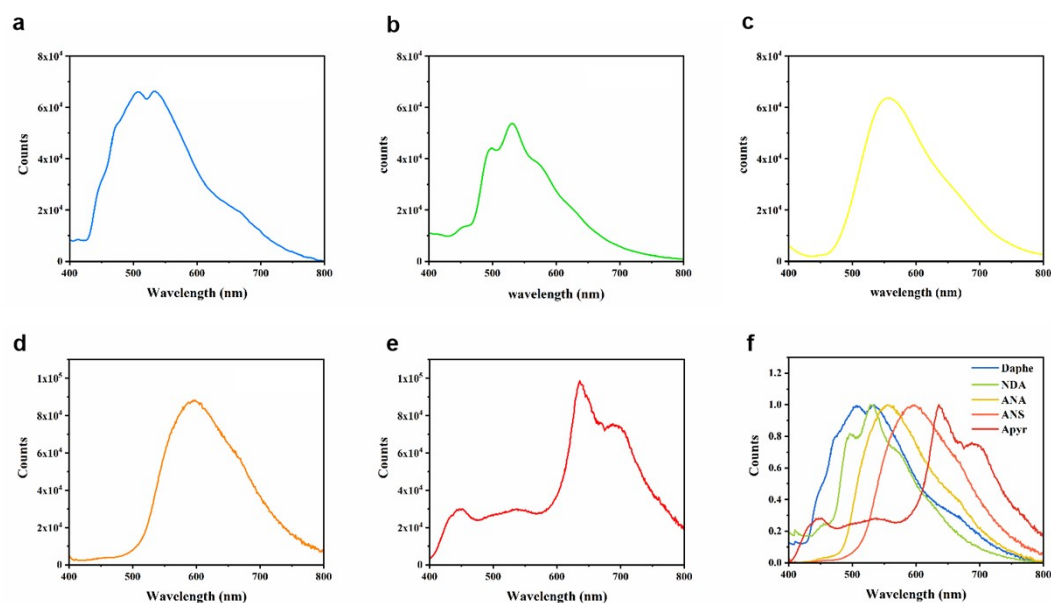
Figure S5. The delayed phosphorescence spectra of five materials taken under 365 nm UV light. (a) Daphe@ε-PL (λem = 508nm), (b) NDA@ε-PL (λem = 530 nm), (c) ANA@ε-PL (λem = 555 nm), (d) ANS@ε-PL (λem = 596 nm), and (e) Apyr@ε-PL (λem = 635nm /693 nm). (f) Summary chart.

As can be seen from Fig. S5, doped guest molecules displayed dispersion states such as monomer, dimer and molecular cluster. Thus, the different aggregation states of doped guest molecules generated different luminescence centers, resulting in wide multiple phosphorescence spectra and different afterglow behavior.

Table S1. Photophysical parameters of ε-PL-based afterglow films under ambient conditions.

	λ_f/nm	λ_p/nm	Φ_s/%	Φ_f/%	Φ_p/%
Daphe@ε-PL	450	473/508/533	4.45	2.77	1.68
NDA@ε-PL	448	596/530	12.82	10.29	2.53
ANA@ε-PL	433	555	18.84	16.99	1.85
ANS@ε-PL	454	596	9.03	8.34	0.69
Apyr@ε-PL	450	635/693	6.60	6.37	0.23

Where, λ_f = the wavelengths of fluorescence; λ_p = the wavelengths of phosphorescence (λ_{ex}=365

nm). Φ_s = quantum efficiency of solid films; Φ_f = fluorescence efficiency; Φ_p = phosphorescence efficiency.
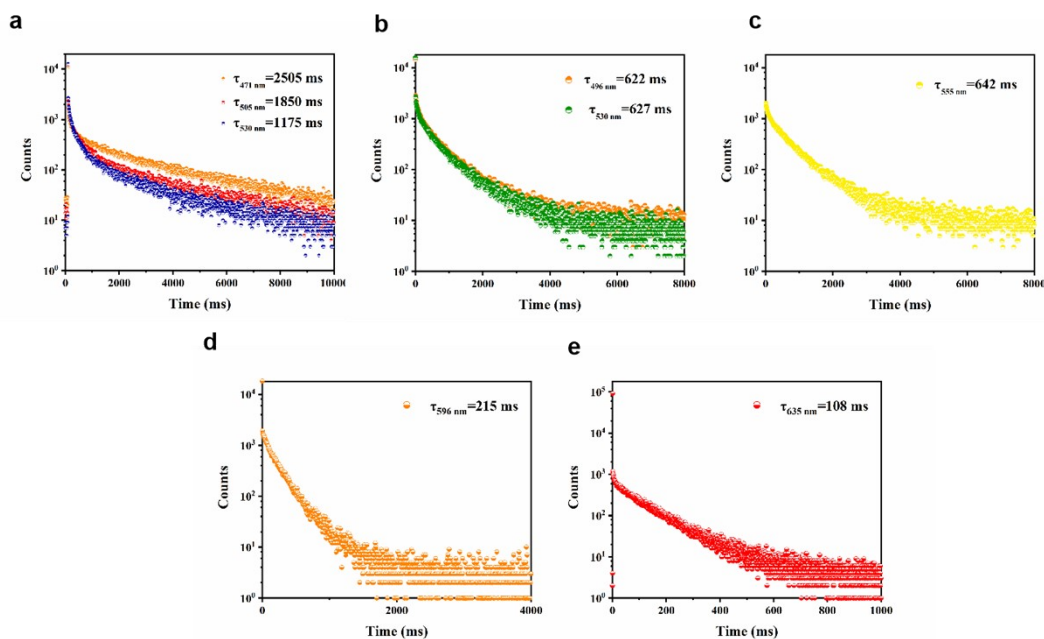

Figure S6. Time-resolved emission attenuation curves of five ε-PL-based films at different wavelengths. (a) Daphe@ε-PL, (b) NDA@ε-PL, (c) ANA@ε-PL, (d) ANS@ε-PL, and (e) Apyr@ε-PL (Daphe@ε-PL was taken under 310 nm UV light and the rest under 365 nm)
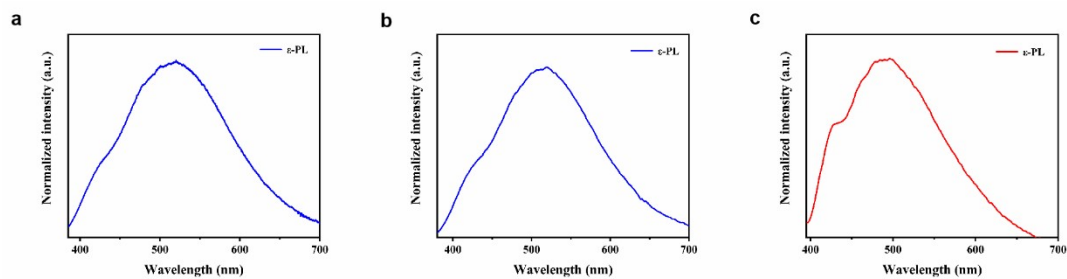

Figure S7. The delayed (t_d=0.1 ms) phosphorescence spectra of ε-PL excited by 365 nm UV light (a) at room temperature, (b) in nitrogen atmosphere, (c) at 77K in solution (10^{-5}M).
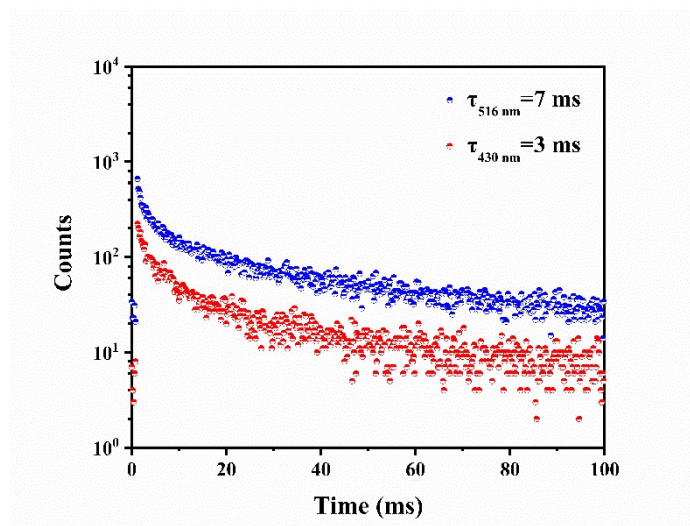
Figure S8. Time-resolved emission attenuation curves of ε-PL films at different wavelengths taken under 365 nm UV light.
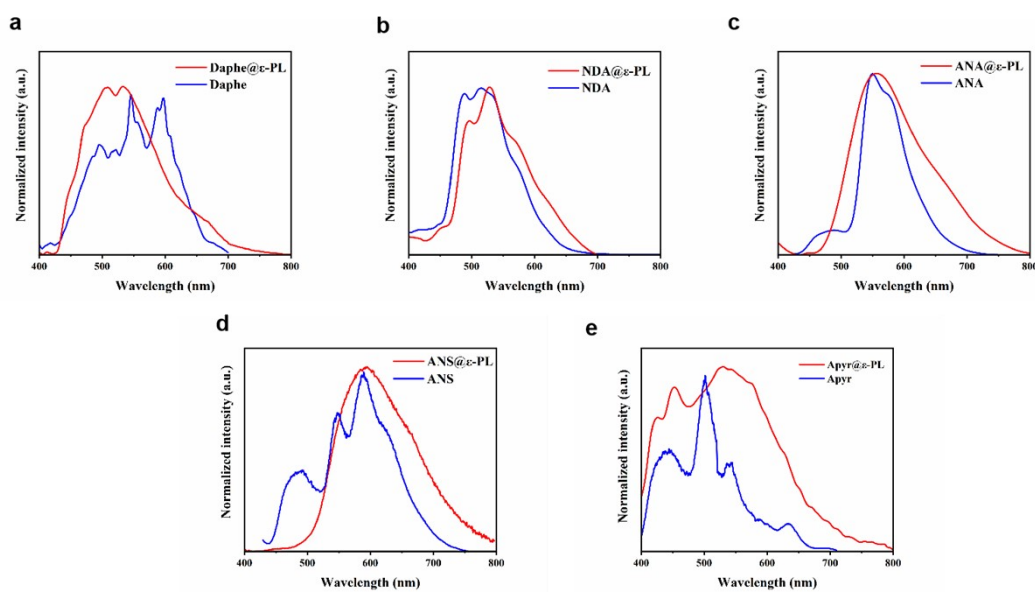

Figure S9. Normalized delayed PL spectra of ε-PL-based afterglow films at 77K (a) Daphe in 2-methyltetrahydrofuran and Daphe@ε-PL, (b) NDA in ethanol and NDA@ε-PL, (c) ANA in ethanol and ANA@ε-PL, (d) ANS in deionized water and ANS@ε-PL, and(e) Apyr in ethanol and Apyr@ε-PL (Blue is liquid (10^{-5} M) and red is solid).
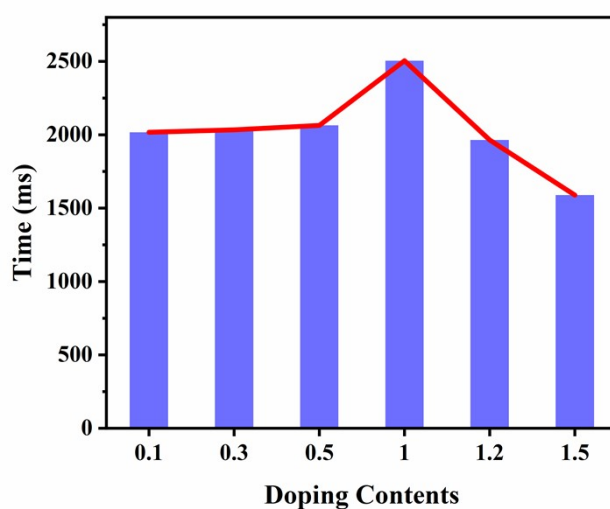
Figure S10. Intuitive image of the lifetime of Daphe@ε-PL at different doping amounts.

Table S2. Photophysical parameters of Daphe@ε-PL films.

	λ_{ex}/nm	λ_f/nm	λ_p/nm	τ/ms
Daphe@ε-PL	254	458	461	2002
Daphe@ε-PL	310	449	471/505/530	2505/1850/1175
Daphe@ε-PL	365	450	508/533	1352/1017

Where, λ_{ex} = excitation wavelength; λ_f = the wavelengths of fluorescence; λ_p = the wavelengths of phosphorescence; τ = afterglow lifetime.
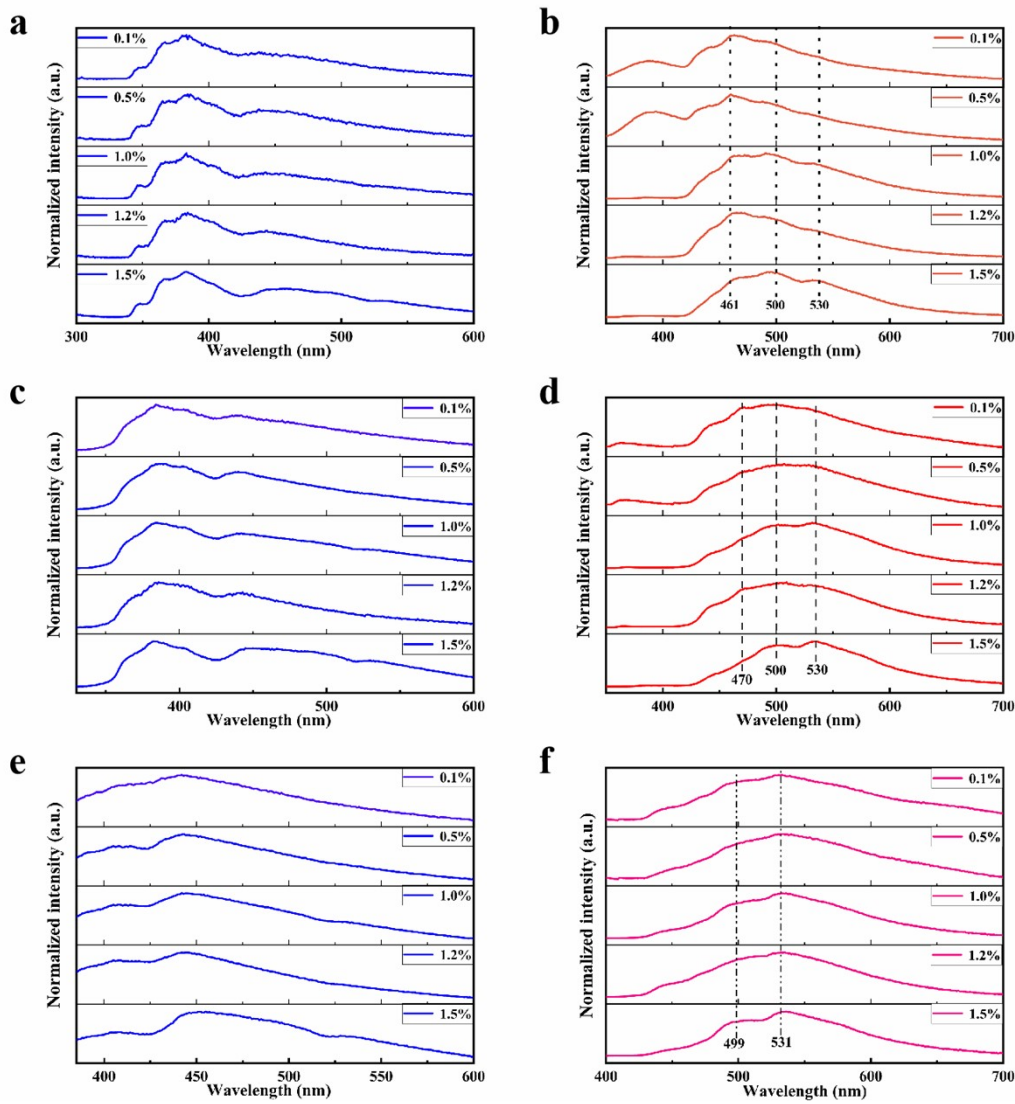
Figure S11. Normalized fluorescence spectra of Daphe@ε-PL films with different doping contents excited by (a) 254 nm, (c)310 nm, (e) 365 nm UV light. Normalized delayed PL spectra of Daphe@ε-PL with different doping contents excited by (b) 254 nm, (d)310 nm, (f) 365 nm UV light.
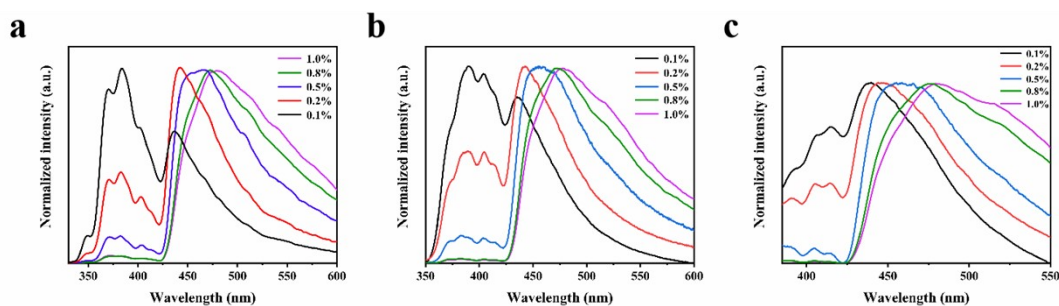
Figure S12. Normalized fluorescence spectra of Daphe@ε-PL in the liquid state with different doping contents excited by (a) 254 nm, (b)310 nm, (c) 365 nm UV light.
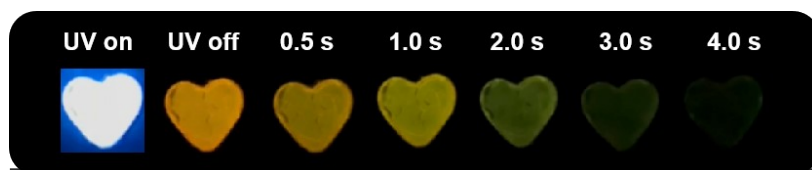

Figure S13. (a) Photographs of ANS@ε-PL films taken under 365 nm UV lights or after ceasing the irradiation.
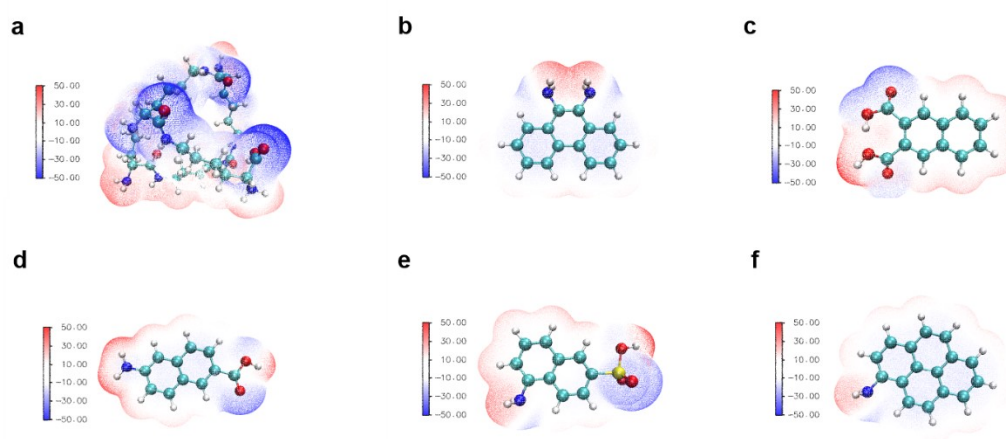

Figure S14. Electrostatic potential distribution on molecular surface. (a) ε-PL. (b) Daphe. (c) NDA. (d) ANA. (e) ANS. (f) Apyr (The negative potential shown in blue and the positive potential shown in red).
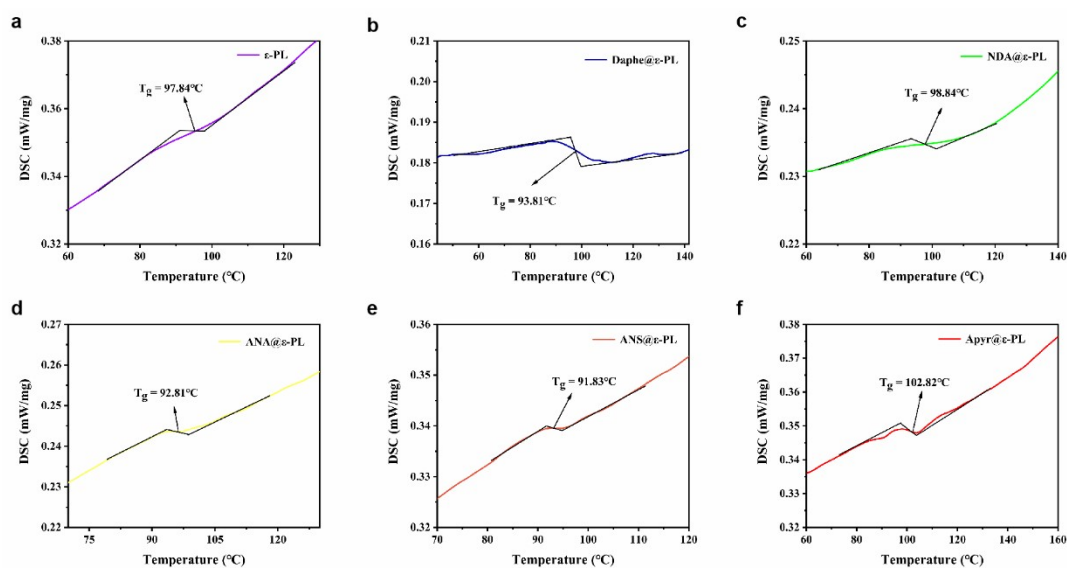
Figure S15. Partial magnification of DSC curves of ε-PL-based RTP films. (a) ε-PL. (b) Daphe@ε-PL. (c) NDA@ε-PL. (d) ANA@ε-PL. (e) ANS@ε-PL. (f) Apyr@ε-PL (T_g was figured out by the isometric method).

T_g was figured out by the isometric method. T_g and the RTP afterglow performances are intrinsically related. The higher the T_g of the material, the better the stability of the material. When the temperature reaches the T_g of the material, the state of the material will be changed, the original rigid environment in the system will be destroyed, and the triplet excitons of the guest molecules will be easily quenched, thus shortening the time of afterglow.

Table S3. the calculated energy levels of Daphe@ε-PL

Excited State	T_1	T_2	T_3	T_4	T_5	S_1	S_2	S_3	S_4	S_5
Energy Level(eV)	2.6891	3.4913	3.5505	3.8232	3.9545	3.9820	4.1998	4.7469	5.0608	5.0666

Table S4. the calculated energy levels of NDA@ε-PL

Excited State	T_1	T_2	T_3	S_1	T_4	T_5	S_2	S_3	S_4	S_5
Energy Level(eV)	2.5994	3.2752	3.8724	3.9251	4.0247	4.0941	4.1280	4.4132	4.6372	4.9608

Table S5. the calculated energy levels of ANA@ε-PL

Excited State	T_1	T_2	T_3	S_1	T_4	S_2	T_5	S_3	S_4	S_5
Energy Level(eV)	2.5667	3.4696	3.5388	3.8492	3.9982	4.0493	4.2454	4.8087	4.9080	5.3169

Table S6. the calculated energy levels of ANS@ε-PL

Excited State	T_1	T_2	T_3	T_4	S_1	T_5	S_2	T_6	S_3	T_7
Energy Level(eV)	2.6855	3.8678	4.0800	4.1820	4.2716	4.4361	4.4602	4.6477	4.7009	5.2533

Table S7. the calculated energy levels of Apyr@ε-PL

Excited State	T_1	T_2	T_3	T_4	S_1	S_2	T_5	S_3	S_4	S_5
Energy Level(eV)	2.0728	3.4119	3.5306	3.5793	3.6602	3.7365	3.8500	4.1702	4.4153	4.5804
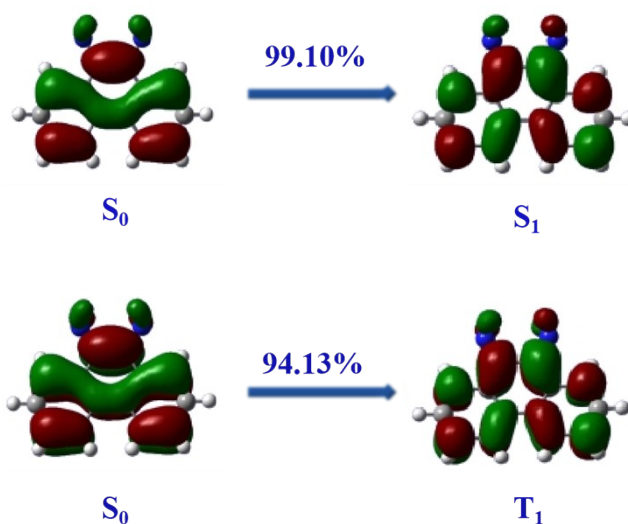
Figure S16. the NTO characteristics of $S_0{\rightarrow}T_1$ and $S_0{\rightarrow}S_1$ transitions of 9, 10-Diaminophenanthrene.
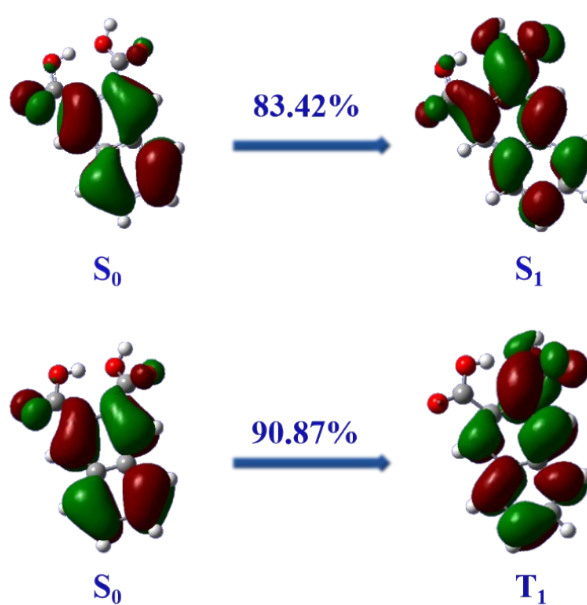

Figure S17. the NTO characteristics of $S_0{\rightarrow}T_1$ and $S_0{\rightarrow}S_1$ transitions of 2, 3-Naphthalenedicarboxylic Acid.
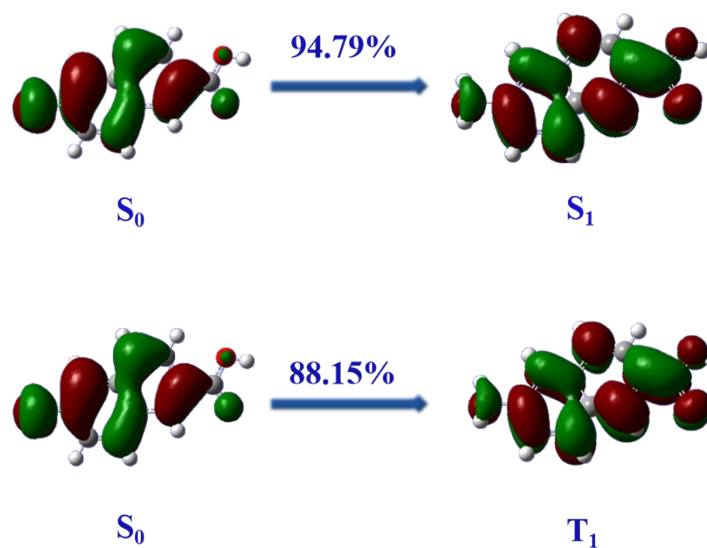
Figure S18. the NTO characteristics of $S_0 \rightarrow T_1$ and $S_0 \rightarrow S_1$ transitions of 6-Amino-2-Naphthoic.
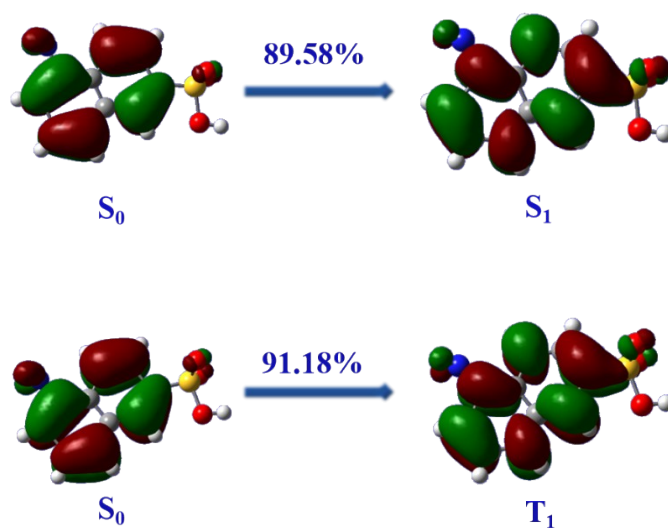

Figure S19. the NTO characteristics of $S_0 \rightarrow T_1$ and $S_0 \rightarrow S_1$ transitions of 6-Amino-2-Naphthoic.
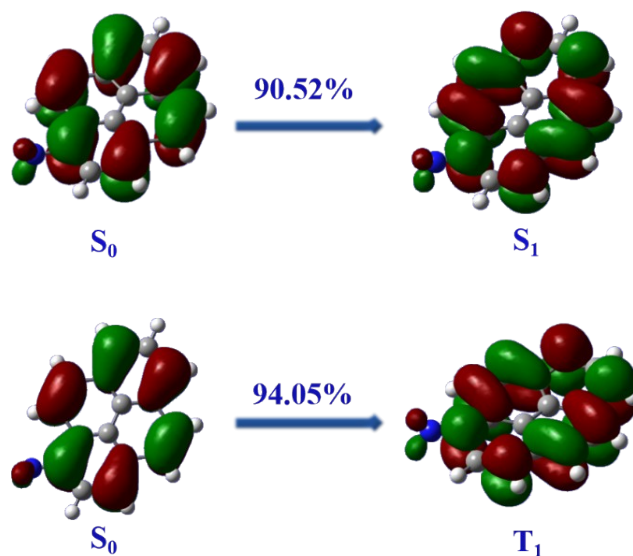
Figure S20. the NTO characteristics of $S_0 \rightarrow T_1$ and $S_0 \rightarrow S_1$ transitions of 1-Aminopyrene.
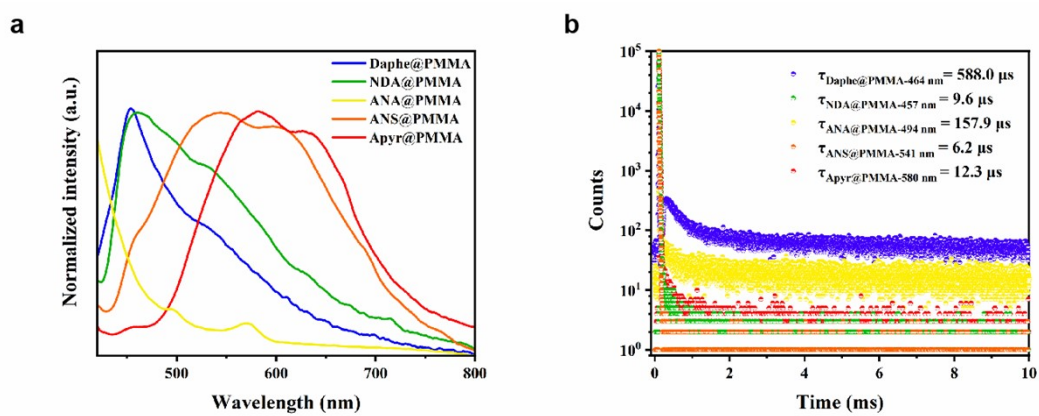

Figure S21. (a) Phosphorescence spectra of PMMA doped small molecules. (b) Time-resolved emission attenuation curves of PMMA-based films at different wavelengths taken under 365 nm UV light.
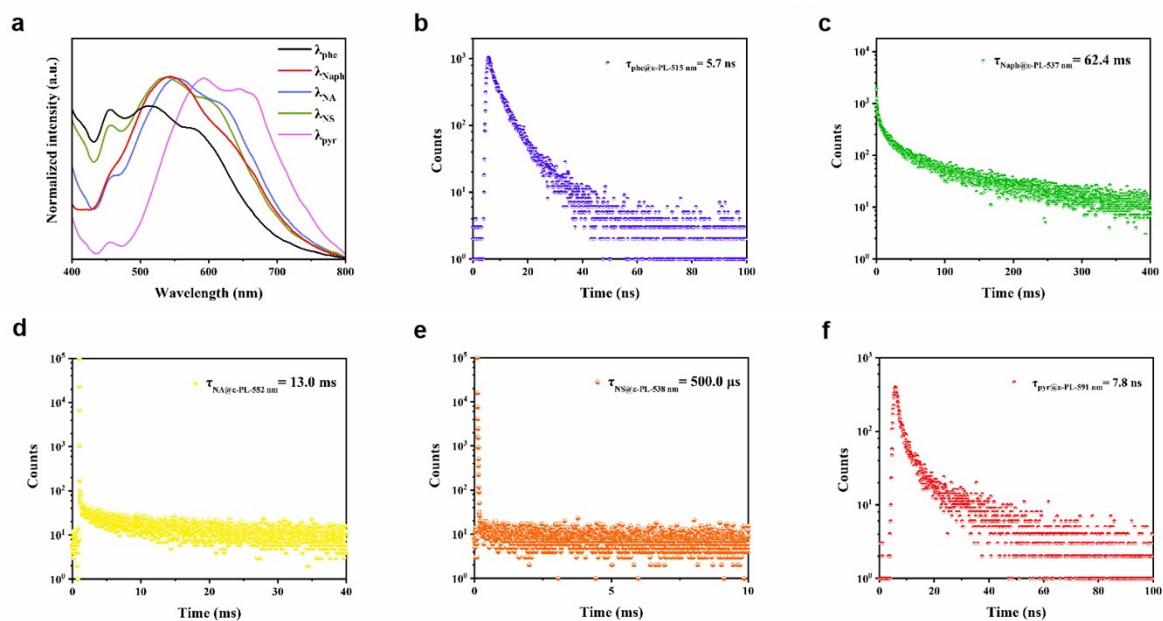
Figure S22. (a) Phosphorescence spectra of ε-PL-based afterglow films doped small molecules without amino and carboxyl groups. (b-f) Time-resolved emission attenuation curves of ε-PL-based films doped with (b) phenanthrene (phe), (c) naphthalene (Naph), (d) 2-naphthalic acid (NA), (e) 2-naphthalene sulfonic acid (NS) and (f) pyrene (pyr) at different wavelengths taken under 365 nm UV light.
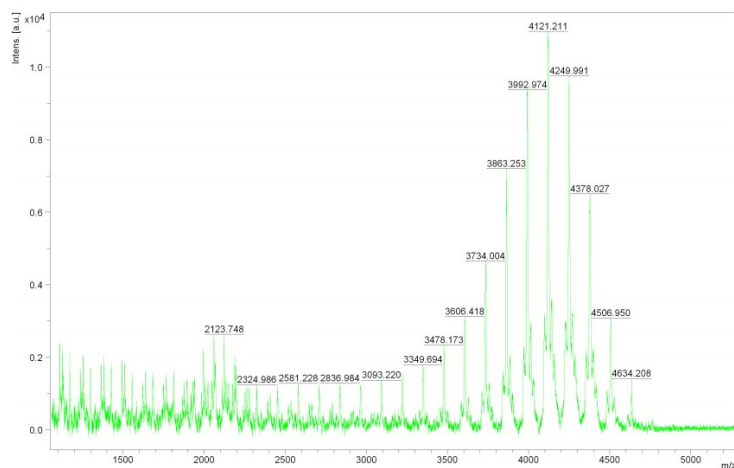

Figure S23. High resolution mass spectrum of pure ε-PL.

It can be seen from the mass spectrum that the molecular weight of ε-PL is about 4121 (The molecular weight range of ε-PL purchased is 3800-4200). Since the molecular weight of the monomer of ε-PL is 116, it is obtained that the degree of polymerization of ε-PL is about 36.